One-step Real-time Food Quality Analysis by Simultaneous DSC–FTIR Microspectroscopy

Shan-Yang Lin* and Chih-Cheng Lin

Department of Biotechnology, Yuanpei University,

Hsin-Chu, Taiwan, ROC.

***Corresponding author**

Prof. Shan-Yang Lin, Ph.D.

Department of Biotechnology,

Yuanpei University, Hsin Chu, Taiwan, ROC.

E-mail: sylin@mail.ypu.edu.tw

ACCEPTED MANUSCRIPT

Table of Contents

1. Introduction-Quality and Stability of foods.

2. Instrumentations for food analysis

3. Novel DSC-FTIR microspectroscopic technique

4. DSC-FTIR microspectroscopy applied in the food sciences

4.1 Rapid evaluation of squid oil stability

4.2 Cooking simulation and quick detection of the degraded product of aspartame

4.3 Fast evaluation of dehydration/rehydration cycle of trehalose

4.4 One-line monitoring glucose/asparagine Maillard reaction

5. Conclusions and future trends

Acknowledgements

References

Abstract

This review discusses an analytical technique that combines differential scanning calorimetry and Fourier-transform infrared (DSC–FTIR) microspectroscopy, which simulates the accelerated stability test and detects decomposition products simultaneously in real time. We show that the DSC–FTIR technique is a fast, simple and powerful analytical tool with applications in food sciences. This technique has been applied successfully to the simultaneous investigation of: encapsulated squid oil stability; the dehydration and intramolecular condensation of sweetener (aspartame); the dehydration, rehydration and solidification of trehalose; and online monitoring of the Maillard reaction for glucose (Glc)/asparagine (Asn) in the solid state. This technique delivers rapid and appropriate interpretations with food science applications.

Key words:

DSC-FTIR, Food Quality, Stability, squid oil, aspartame, DKP, trehalose,

Maillard reaction

1. Introduction - quality and stability of foods

Food is a well-known complex system that contains carbohydrates, proteins, lipids, minor components and water, and it can take many different forms (Damodaran et al., 2007; Belitz et al., 2009; Coultate, 2009). Maintaining quality throughout food chains is a key issue affecting the food industry. Several phases and compounds coexist in the metastable conditions of food while microbes may also be present. Thus, food must be protected from physical and chemical instabilities such as phase separations in dispersed systems, phase transitions, enzymatic reactions and ingredient degradation, as well as microbial contamination during processing, packaging, shipping, handling and storage (Skibsted et al., 2010**)**. The physicochemical properties and stability of food are strongly dependent on its composition and storage conditions, so quality control is of vital importance in food production. Food quality control plays a significant role in ensuring the supply of high quality, safe and nutritious food to the public, which promotes their good health and delivers economic benefits (Alli, 2003; Clute, 2008).

In general, food quality control is based on technological, physical, chemical, microbiological, nutritional and sensory parameters that indicate wholesome foods. The stability and shelf life of a food product are critical for its possible success in the market, so food stability is a unique approach for understanding this critical area based on an examination of the physical, chemical and biochemical factors that affect food quality (Eskin and Robinson, 2000**)**. Accelerated testing is used widely to predict the storage stability and quality of labile products (Franks, 1994). The prediction of the shelf life of food products is based on the application of the principles of temperature-dependent chemical reaction kinetics. Reaction rates depend on the product

compositions and environmental factors such as the temperature, humidity and atmospheric conditions (Valentas et al., 1997). Food, pharmaceutical and bioindustry products are stressed by testing at high temperatures. The thermal properties of food systems are important for understanding the relationship between food properties and food quality. In general, an increase in temperature will increase the rate of chemical reactions, thereby accelerating deterioration. If food contains fats, more solid fats will enter their liquid phase and act as a solvent to accelerate reactions that occur in the liquid-oil phase. Changes in fat crystallinity may also occur. Temperature increases can also affect the recrystallization of sugar syrup in foods, which may modify food matrices (Kilcast and Subramaniam, 2000)..

To ensure the quality and safety of foods, food companies need to meet the expectations of consumers. Thus, a total quality management (TQM) system must be implemented in all areas. Food quality control should be directed at different levels and different analytical methods and procedures should be established for all production steps. The analytical methods used for quality control need to be changed to meet the demands of the consumers, manufacturers and researchers and to satisfy legislative policy. Simple methods based on chemical, physical and biochemical/immunological principles are commonly used for routine analysis, although two or more combined methods may be the method of choice (Muller and Steinhart, 2007; Paré and Bélanger, 1997**)**.

2. Instrumentation used for food analysis

The detection and characterization of the physical and chemical properties of food materials are essential for ensuring the quality and safety of marketed food products during development and commercialization. There is a need for the continuous application and development of reliable analytical techniques in food science. The reliability of these methods is determined using a validation procedure. This requires verification of the specificity, accuracy, precision (repeatability and reproducibility), detection limit, sensitivity, applicability and practicability of a technique, as appropriate. Indeed, any analytical technique used for food analysis depends on the study aims of a scientist and/or the food property selected by the manufacturer or customer. Analytical techniques may cover a broad range of methods such as chromatographic, spectroscopic, electroanalytical and electrophoresis techniques, as shown in Table I (Ibañez and Cifuentes, 2001) based on the complexity of the food matrices .

The complexity of the food matrix, the high probability of interference and the low analyte concentration in food products may demand that coupled techniques are used to overcome these problems (Ibañez and Cifuentes, 2001). The coupling of techniques such as liquid chromatography–mass spectrometry (LC–MS), gas chromatography–mass spectrometry (GC–MS) and gas chromatography–Fourier transform infrared spectrometry (GC–FTIR) are well established in food sciences and they are considered to be mature routine techniques. Recently, food authentication has becoming increasingly important in the food industry. Powerful coupled techniques are now used more widely to ensure food authenticity and these methods have their own strengths and limitations (Cordella et al., 2002; Ibañez and Cifuentes, 2001).

In 1986, Mirabella first introduced a combination of differential scanning calorimetry (DSC) and FTIR microspectroscopy to study polymer melting directly (Mirabella, 1986). Many subsequent studies have focused on the development of a combined apparatus and operational variables. This DSC–FTIR microscopic technique can be used easily and successfully to study the thermal and spectral properties of a material in real time as it undergoes changes (Johnson et al., 1992; Spragg, 2000). This technique is a simple, rapid and powerful tool for testing the thermal-dependent conformational behaviour of microsamples and it is also used for accelerated stability testing to predict the stability and shelf life of samples. In our laboratory, this unique system has been applied extensively for investigating thermal effects on structural change and reactions in samples (Lin and Wang, 2012). However, this DSC–FTIR microscopic system method has been used rarely in food science. This review article discusses the applications of this unique DSC–FTIR microscopic technique in food science.

3. The novel DSC–FTIR microspectroscopic technique

Cooking, one of the most common thermal treatments applied during food processing, improves the palatability, digestibility and keeping quality of food (Kaletunc, 2009). Understanding the thermal and functional properties of food components and ingredients during thermal treatments is of great importance for food science research and food quality assurance. DSC is one of the most commonly used thermal analyses in food science, which measures the thermodynamic and thermal properties of food, such as the freezing point, melting point, phase transitions and enthalpy. The DSC approach to food analysis is similar to food cooking; however, DSC can detect simultaneous thermal changes during the heating process. Thermal analysis is used as a

research tool by analysts, but it is also a real-time monitoring technique for studying process-induced changes (Farid, 2010).

DSC is used frequently to determine information about the thermal properties of the materials but the main chemical functional characterizations of materials is generally determined by FTIR spectroscopy. The combination of DSC and FTIR allows the determination of simultaneous thermal and spectral data for the same test sample during a single experiment in real time. The DSC–FTIR technique yields simultaneous thermodynamic and spectroscopic information about a solid or liquid sample undergoing thermal modification (Akinade et al., 1994; Johnson et al., 1992; Ziegler et al., 1995). The coupling of DSC and FTIR in a single system implies that DSC can measure the exothermic and endothermic responses of samples, while the FTIR analysis observes changes in their chemical and physical composition at the same time.

A schematic of the DSC–FTIR microspectroscopic apparatus and its IR beam path is shown in Fig. 1. Simultaneous DSC and FTIR experiments have generally involved the use of a miniature DSC positioned under the objective of an IR spectrometer, which is coupled to a microscope. The DSC cell is usually mounted on a microscope stage. In our laboratory, the FP84HT hot stage is used as a DSC cell, which provides a precise thermal measurement cell for simultaneous visual observation and heat flow measurements (Fig. 2). In the instrumental configuration, the IR beam passes through a hole in the DSC cell via the IR microscope to the MCT detector. The sample is placed in a hole in the DSC cell, which uses the transmission or reflectance mode. A careful alignment procedure is required prior to operation. This unique DSC–FTIR microspectroscopy

approach is a simple, quick and timesaving tool, which delivers fast performance in a one-step continuous process and it also simultaneously correlates the thermal response and the IR spectra during structural changes in samples. This DSC–FTIR measurement procedure may be used to analyze different samples such as solids, films and solutions using the transmission or reflectance mode.

4. Application of DSC–FTIR microspectroscopy in food sciences

4.1 Rapid evaluation of squid oil stability

Fish oil is a rich source of eicosapentaenoic acid (EPA) and docosahexaenoic acid (DHA), which are polyunsaturated fatty acids (PUFAs) that are beneficial to human health (Halim and Newby, 2012; Lee et al., 2009) The quality of fish oil depends greatly on the type of fish from which the oil is derived. However, the presence of long chain PUFAs in fish oils makes this oil susceptible to oxidation, which affects various properties of the fish oil such as its sensory quality, nutritional value, functionality and toxicity (Taneja and Singh, 2012; Chaiyasit et al., 2007; Boran et al., 2006; Maqsood et al., 2012) This oxidation process may be accelerated when oils are subjected to different temperatures during various operation processes. This may have severe health consequences after the regular intake of putrefied/rancid oils, possibly to cause the free radicals production and have cytotoxic and mutagenic effects in the human body (Kubow, 1990; Perjési et al., 2002; Ragnarsson and Labuza, 1977).

In general, an oil sample is readily oxidized when subjected to air or oxygen flow, heating, light or catalysts (Fereidoon, 2005). Vlachos et al. heated corn oil for 30 min at various temperatures

during an oxidation experiment (Vlachos et al., 2006). Based on the FTIR spectra, they found that the band at 2854 cm^{-1} (symmetric CH_2 stretching) and the shoulder at 2962 cm^{-1} (symmetric CH_3 stretching) had an increased intensity whereas the band at 2925 cm^{-1} (asymmetric CH_2 stretching) had a lower absorbance, while there was a wider 'valley' between the 2925 and 2854 cm^{-1} bands with increased temperature. In addition, a shoulder at 2872 cm^{-1} (asymmetric CH_3 stretching) was observed. A baseline shift was also observed, which indicated that oxidation occurred in the heated corn oil. An antioxidant from oregano was then added to corn oil and it was heated at 245°C for 30 min. However, the valley produced by the corn oil with oregano was exactly the same as that produced by the oregano-free corn oil kept at 25°C, suggesting the antioxidant activity of oregano (Lagouri and Boskou, 1996).

Squid liver oil extracted from fresh squid is a food product that contains an abundance of DHA and EPA. It is also a vital dietary supplement that confers health benefits (Rossi et al., 2011; Swanson et al., 2012). However, it is vulnerable to oxygen because of its high degree of unsaturation, which limits its usage in foods (Lin and Hwang, 1993; 2002). The degradation products of PUFA after oxidation also generate an off flavour and their excess ingestion may be hazardous to human health (Gonzalez, 1995; Staprans etal., 2005).

Thus, the stabilization of squid oil during the manufacturing process and storage is an important issue in the food industry. We successfully used a spray drying technique to encapsulate and stabilize squid oil (Lin et al., 1995a; 1995b). To determine the thermal stability of unencapsulated or encapsulated squid oils in different thermal conditions, we used DSC–FTIR to

estimate the encapsulation efficiency of several hydrophilic macromolecules that were used as capsule wall materials. Figure 3 shows a three-dimensional plot of the FTIR spectra of unencapsulated or encapsulated squid oil samples between 1700 and 1800 cm^{-1} as a function of temperature. The major peak at 1747 cm^{-1} was assigned to C=O in the ester group of lipids. This clearly shows that the peak intensity near 1747 cm^{-1} became weaker with an increase in temperature with unencapsulated (A) and encapsulated (B) squid oils, which was mainly due to the degradation of squid oil. The peak intensity showed a less decrease with the unencapsulated squid oil compared with that of the encapsulated squid oil. The change in peak intensity at 1747cm^{-1} with temperature is shown in Fig. 3-C. It was apparent that squid oil microcapsules prepared via a specific formulation of hydrophilic macromolecules had a significantly reduced decreasing trend in the peak intensity. The unencapsulated oil began to degrade at 30°C with almost no induction period, whereas the encapsulated oils prepared by a specific formulation containing gelatin, sodium caseinate, maltodextrin, lecithin and Avicel had a long induction period until about 160°C. This indicates that the microencapsulation technique effectively protected squid oil from thermal degradation. Thus, DSC–FTIR microspectroscopy appears to be a useful tool for determining temperature-induced changes in the molecular structure of samples.

4.2 Cooking simulation and rapid detection of the degradation product of aspartame

Aspartame (APM) is a white crystalline powder that is manufactured from two amino acids, phenylalanine and aspartic acid. APM is an artificial sweetener used in over 6000 products worldwide and it is used increasingly in foods, beverages and pharmaceuticals. The U.S. Food and Drug Administration and European Food Safety Authority have established acceptable daily

intake levels of 50 and 40 mg kg^{-1} bw day^{-1} of APM (Butchko and Stargel, 2001; Magnuson et al., 2007). Magnuson et al. indicated that APM is safe at current levels of consumption as a non-nutritive sweetener based on the weight of existing scientific evidence, but APM may be hydrolyzed into its constituent amino acids including phenylalanine, which is not metabolized by people with the genetic disorder phenylketonuria (PKU). Thus, APM-containing foods and beverages must carry a label to alert people with PKU (Magnuson et al., 2007). Furthermore, APM and its by-product diketopiperazine (DKP) have been implicated in the possible occurrence of carcinogenicity in Sprague–Dawley rats, although other studies provide no evidence to support an association between aspartame and cancer in any human tissues (Magnuson et al., 2007; Soffritti et al., 2006).

The taste and quality of many APM-containing foods and beverages depends on the physical and chemical properties of APM, so the stability of APM plays a critical role in these products. The stability of APM depends on time, temperature, pH and water activity (Dziezak, 1986; Bell and and Hageman, 1994; Bell and Labuza, 1991a and 1991b; Huang et al., 1987). Thus, the stability and shelf life of APM should be well understood before attempting different formulation designs. In particular, APM is vulnerable to heat, which limits its use as a sugar replacement during baking or cooking. The thermal instability of APM increases with temperature during a specific storage time (Leung and Grant, 1997; Bell and Hageman, 1994). Fellows et al. reported that increased temperature might accelerate the degradation of APM in the fruit preparations used in yoghurt production (Fellows et al., 1991).

APM usually exists as a hemihydrate in commercial raw materials, although there are two hemihydrate polymorphs (Leung et al., 1998a and 1998b). Upon heating, both hemihydrate polymorphs may dehydrate to produce an anhydrate and they yield 3-(carboxymethyl)-6-benzyl-2,5-dioxopiperazine (DKP) via a cyclization reaction at higher temperatures. The DSC curve of an APM hemihydrate is shown in Fig. 4 (Lin and Cheng, 2000). Clearly, there are three endothermic peaks near 123, 181 and 240°C. The TGA curve demonstrating four losses in weight is also shown in Fig. 4. The first 1.69% weight loss in the TGA curve was due to the evaporation of adsorbed water. The first DSC endothermic peak at 123°C and its TGA weight loss from 110°C (1.68%) might be due to dehydration of the hemihydrate in the APM lattice. The second DSC endothermic peak at 181°C and its corresponding TGA curve from 153°C (13.10%) were attributed to the intramolecular cyclization of APM molecules to form DKP (Leung et al., 1998a; Leung and Grant, 1997; Lin and Cheng, 2000; Cheng and Lin, 2000; Lin and Wang, 2012). The third DSC peak at 240°C and its related TGA weight loss from 223°C were attributed mainly to the melting of DKP, which was formed as an impurity of APM, and it mixed with the uncyclized APM to broaden the melting range. The degradation of APM started from 240°C and its weight loss to 300°C was about 29.03% (Lin and Cheng, 2000).

However, the identification of solid-state DKP formation at 181°C required several complex, indirect and time-consuming analytical steps including thermal pretreatment, separation techniques and HPLC analysis (Prodolliet and Bruelhart, 1993; Skwierczynski and Connors, 1993; Berset and Ochsenbein, 2012; Pattanaargson and Sanchavanakit, 2000; Sabah and Scriba,

1998). In contrast, our simultaneous DSC–FTIR microscopic system facilitated the rapid and direct investigation of the dehydration process pathway and the identification of the degraded APM product in the solid state. A continuous pathway of water evaporation, dehydration and intramolecular cyclization were detected readily using our one-step DSC–FTIR microspectroscopic analysis (Lin and Cheng, 2000; Cheng and Lin, 2000).

(1) APM water evaporation and dehydration processes

Figure 5 shows three-dimensional plots of the FTIR spectra of APM in the ranges 3450–3200 cm^{-1} (A) and 1700–1300 cm^{-1} (B), with an increase in temperature from 25 to 120°C. Figure 6 shows the thermal-dependent pathway of APM. About 3.37% of the water was contained in APM molecules, including absorbed water and hemihydrate (Fig. 4), so the IR peaks at 3315 (hydrogen bonded NH), 1585 and 1367 (asymmetric or symmetric COO^-) cm^{-1} were attributed to the hydrogen bonding between water, NH_3^+ and COO^- in APM, respectively (Fig. 6-A). As the temperature rose beyond 50°C, the three peaks at 3315, 1585 and 1367 cm^{-1} gradually disappeared due to the loss of absorbed water (Fig. 6-B), which also reduced the hydrogen bonding between adsorbed water and the APM molecules. However, the peaks at 3338 and 1627 cm^{-1} were also observed at the same time. The IR peak at 3338 cm^{-1} was assigned to free NH stretching of amine in the APM molecule while the peak at 1627 cm^{-1} was related to free water embedded within the KBr disc.

As the temperature reached above 110°C, the IR peak at 1627 cm^{-1} disappeared, suggesting the complete loss of free water from the KBr pellets. At the same time, the IR peaks at 1662 and

1549 cm^{-1} shifted to 1666 and 1543 cm^{-1}, respectively. The peaks at 1362 and 1331 cm^{-1} gradually appeared after 110°C. The shift of the IR peaks above 110°C may have been attributable to the hydrogen-bonded C=O and N–H in amides I and II of the APM molecule, which changed to free C=O and free N–H, as well as the dehydration of hydrate embedded in the molecular packing of the APM crystal lattice (Fig. 6-C). The appearance of IR peaks at 1362 and 1331 cm^{-1} from 110°C also explained the increase in the free -COOH in the APM molecule due to the gradual loss of hydrogen bonding after dehydration of the hydrate. Thus, the microscopic DSC–FTIR system analyzed the process of the evaporation of free adsorbed water and the dehydration of hemihydrate from APM molecules in real time.

(2) Intramolecular cyclization of the APM molecule

APM can also form DKP, which is an impurity of APM, via intramolecular cyclization. However, this is usually difficult to demonstrate without using complex analytical procedures. The DSC–FTIR analysis generated the temperature-dependent three-dimensional plots of the FTIR spectra of APM at 3450–2700 cm^{-1} (C) and 1800–1160 cm^{-1} (D) in the temperature range from 120 to 200°C (Fig. 5). The peak at 3338 cm^{-1} (free NH stretching) disappeared after 174°C, whereas two new peaks were observed at 3203 and 3088 cm^{-1} (NH stretching of DKP). Moreover, the peak at 1736 cm^{-1} (carbonyl group of ester) disappeared gradually from 153°C whereas a new peak increased slowly at 1718 cm^{-1} (C=O of carboxylic acid). The peak at 1666 cm^{-1} (amide C=O) also shifted to 1670 cm^{-1} (C=O of DKP) with a higher intensity because two diketones were present in the DKP ring. An outline of the intramolecular cyclization pathway of the APM molecule above 153°C is shown in Fig. 6-D. The amide II-related NH peak at 1543

cm^{-1} also disappeared after 174°C, which was possibly due to the complete formation of DKP. The peaks at 1377 and 1225 cm^{-1} (methyl group and C=O of ester) disappeared after the liberation of methanol from the APM molecule, while the peak at 1283 cm^{-1} (CN of DKP) appeared gradually. Clearly, the DSC–FTIR microscopic system could analyze the thermal-dependent structural rearrangement of the APM molecule via intramolecular cyclization. This provides a powerful illustration of the use of the DSC–FTIR microscopic technique as a potential tool for simulating the cooking process and analyzing the degradation products of APM in real time.

4.3 Rapid evaluation of the dehydration/rehydration cycle of trehalose

Trehalose is a well-known natural disaccharide that is formed via a 1,1 linkage of two α-glucose units (Khan et al., 2012). It is accepted as a safe food and an ingredient in the U.S. and the E.U. Trehalose has a powerful ability to suppress bitterness, stringency, harsh flavours and odours in raw foods, meats and packaged foods (Takanobu, 2002; Ohtake and Wang, 2011). It is interesting that trehalose can also protect organisms from various stresses, such as drying, freezing and osmopressure because it possesses a high water retention capacity (Takanobu, 2002; Ohtake and Wang, 2011; Sola-Penna and Meyer-Fernandes, 1998; Elbein et al., 2003). Trehalose is known to play an important role in desiccation tolerance via water replacement or intracellular glass formation during long-term storage in a variety of cells, tissues and possibly organs in a dry state (Sakurai et al., 2008; Elbein et al., 2003). Anhydrobiotic organisms with high trehalose content can survive dehydration for a long period and activity can be restored within minutes of

rehydration. Crowe et al. suggested that both of these activities are required for stabilizing effects in anhydrobiotic systems and that trehalose can fulfil both functions (Crowe, 2007).

Many studies have examined the desiccation tolerance of anhydrobiotic systems in the presence of trehalose, although the actual functional mechanisms underlying the action of trehalose in these systems remain unclear. The dehydration behaviour of trehalose is of particular interest and it has been studied extensively because of its possible relevance to the desiccation tolerance of anhydrobiotic organisms (Furuki et al., 2009; Sussich et al., 2001). Lin and Chien used DSC–FTIR microspectroscopy to simulate and investigate the polymorphic transition of trehalose dihydrate during dehydration, rehydration and solidification processes using a special sample preparation technique (the 1KBr or 2KBr pellet methods) (Lin and and Chien, 2003).

(1) Thermal dehydration of trehalose dihydrate

Figure 7 shows the thermal-dependent FTIR spectra of trehalose dihydrate prepared using the 1KBr method (smearing sample on a KBr disc) or the 2KBr method (sealing a sample between two KBr discs). In the temperature range between 1800 and 900 cm^{-1}, the contour profiles of the IR spectra changed markedly near 67°C with the 1KBr sample and at 64°C with the 2KBr sample. Figure 7 shows a peak at 1687 cm^{-1} (bending vibration of solid-like water in hydrate), several peaks below 1500 cm^{-1} (O–C–H, C–C–H and C–O–H deformation/C–C and C–O stretching) and two peaks at 998 and 957 cm^{-1} (glycosidic bond). (Devlin, 1990; Akao et al., 2001)

The peak intensity at 1687 cm^{-1} decreased sharply for the 1KBr sample at 67°C due to direct dehydration (Fig. 7-A). At the same time, an IR peak at 1640 cm^{-1} appeared quickly at 67°C but disappeared at 79°C. The thermal-dependent spectral changes at 1687 cm^{-1} and 1640 cm^{-1} with the 2KBr sample were similar to those with the 1KBr sample. However, the dramatic temperature change with the 2KBr sample occurred at 64°C, while the peak intensity at 1640 cm^{-1} remained constant after 64°C (Fig. 7-B). Water dehydrated from the dihydrate crystal may have been sealed between the two KBr discs, resulting in the appearance at 1640 cm^{-1} due to the bending of H–O–H. However, the water was evaporated completely from the 1KBr disc at 79°C and the IR peak at 1640 cm^{-1} was absent. Figure 8 shows the thermal-dependent changes in the IR spectral range at 1500–1800 cm^{-1} for trehalose dihydrate prepared using the 2KBr method. The declining peak at 1687 cm^{-1} and the rising peak at 1640 cm^{-1} were observed simultaneously. The water molecules in the trehalose dihydrate crystal underwent a thermal transition from a solid to a liquid state (Akao et al., 1998; Giguere, 1987).

(2) Rehydration of trehalose dihydrate

Isothermal FTIR time-scan measurements were performed to explore the rehydration and solidification processes of trehalose anhydrate. Trehalose dihydrate was prepared using the 1KBr method and preheated to 81°C, cooled to 25°C and analysed isothermally at 25°C with 70% RH for 120 min. Figure 9 shows the isothermal three-dimensional FTIR spectra. The two peaks at 1640 cm^{-1} and 1687 cm^{-1} were clearly changed, whereas the other peaks retained their original shape. Under these isothermal conditions, the peak at 1640 cm^{-1}, which represented the bending band of liquid water, decreased as the thermal treatment period increased. By contrast, the 1687

cm^{-1} peak, which represented solid-like water, increased as the thermal treatment period increased. Both lines tended to equilibrate beyond 70 min but they were almost constant after 100 min. The isothermal conditions (25°C and 70% RH for 120 min) probably induced the rehydration process, which transformed liquid water to solid-like water in trehalose dihydrate. This DSC–FTIR microspectroscopic study facilitated the critical analysis of dehydration and rehydration processes in trehalose.

4.4 Online monitoring of glucose/asparagine in the Maillard reaction

The Maillard reaction is a famous non-enzymatic browning reaction found in the food industry (Chuyen, 1998; Yaylayan and Stadler, 2005). It is responsible for the production of the aroma, taste and colour of various foods in traditional processes such as the roasting of coffee and cocoa beans, the baking of bread and cakes, the toasting of cereals and the cooking of meat (Martins et al., 2001). The first reaction scheme in the general pathway of the Maillard reaction was described by Hodge (Hodge, 1953). Several advanced reactions have been reported in the Maillard reaction, including cyclization, dehydration, retroaldolization, rearrangement, isomerisation and further condensations. The formation and pathways of intermediates and melanoidins have been determined using numerous analytical methodologies, such as high-performance liquid chromatography, MALDI-TOF or proton transfer reaction mass spectrometry and pyrolysis gas chromatography mass spectrometry (Rosén and Hellenäs, 2002; Pollien et al., 2003; Fay and Brevard, 2005; El-Ghorab et al., 2006). However, these sophisticated operations require integrated reaction, separation and identification processes, which are time-consuming. Thus, we applied simultaneous DSC–FTIR microspectroscopy to

explore the continuous Maillard reaction pathways of the solid-state glucose (Glc)/asparagine (Asn) system (Hwang et al., 2012).

Figure 10 shows the thermal-dependent three-dimensional FTIR spectral plot (A) and changes in several specific IR peak intensities (B) for a physical mixture of Glc–Asn. The DSC curve of the Glc–Asn physical mixture is also indicated. This figure clearly shows that the IR spectral contour profile was almost constant below 53°C (Fig. 10-A and B). Above 53°C, several IR peaks began to change their intensities. Above 94°C, there were marked changes in the IR peak intensities at 2363, 1665 and 1711 cm^{-1}. In particular, the peak intensity at 2363 cm^{-1} increased with temperature from 94 to 145°C (Fig. 10-B), before decreasing. The IR peaks at 2363 cm^{-1} might be responsible for the formation of CO_2 via the decarboxylation of the sample (Kulesza et al., 2006). All of the changes in the FTIR spectral contours could be observed directly in the thermal-dependent three-dimensional FTIR spectral plot. Each component of the FTIR spectrum at a specific temperature in Fig. 10-A was compared with that in Fig. 11. Clearly, the same IR spectra were observed in the samples while heating from 30 to 65°C, which was almost the same as the IR spectrum of the Glc–Asn physical mixture before heating. However, after continuous heating between 117–135°C, the peaks assigned to Asn at 1682 and 1644 cm^{-1} were shifted to 1665 and 1629 cm^{-1}. A new peak also appeared at 1724 cm^{-1}. The appearances of both peaks at 1724 (νC=O of COOH) and 1665 (νC=O of $CONH_2$) cm^{-1} were similar to those of the IR spectral peaks at 1726 and 1664 cm^{-1} found in the Schiff base intermediate after the Glc–Asn interaction (Wnorowski and Yaylayan, 2003).

After heating to >117°C, all the IR spectra for the heated Glc–Asn samples were increased markedly. The new peaks at 2363, 2331, 1711, 1660 and 1589 cm^{-1} may be attributed to the formation of new combined products during two processes. The first process was transferred from a Schiff base intermediate to an Amadori product (1660 and 1589 cm^{-1}) while the second process was the formation of CO_2 (2363 and 2331 cm^{-1}) via the decarboxylation of an Amadori product (Wnorowski and Yaylayan, 2003; Kulesza et al., 2006). In particular, the appearance and disappearance of both peaks at 2363 and 2331 cm^{-1} during the heating treatment might strongly suggest that the Amadori rearrangement and decarboxylation from the Schiff base intermediate occurred simultaneously. New IR spectral peaks at 1711, 1643 and 1589 cm^{-1} were observed in the IR spectrum at a temperature of 200°C. These peaks appeared to be related to the IR peaks of the decarboxylated Amadori product (Yaylayan and Stadler, 2005; Yaylayan, 2009). Thus, Figure 12 shows the possible continuous pathway of the solid-state Glc–Asn Maillard reaction that was determined by simultaneous DSC–FTIR microspectroscopy. This model assumes that the solid-state Glc–Asn Maillard reaction forms a Schiff base intermediate initially, before producing an Amadori product and a decarboxylated Amadori product after Amadori rearrangement and decarboxylation (Hoenicke and Gatermann, 2005; Yaylayan, 2009). This study suggests that the continuous pathways used for the formation of the Schiff base intermediate, Amadori product and decarboxylated Amadori product in the solid-state Glc–Asn Maillard reaction could be rapidly analysed simultaneously in real time using our unique one-step DSC–FTIR microspectroscopy technique.

5. Conclusions and future trends

Food quality determines the qualitative characteristics of food that are acceptable for all consumers and higher standards ensure better quality food. The quality of food may consider external characteristics such as sensory properties (appearance and taste) and nutritional value (nutrient content), as well as internal characteristics such as health benefits (functional ingredients) and the material safety (physical, chemical and biological properties) (Earle and Earle, 2003). During any food production process, many stages can affect the quality of the final product and these stages can be identified as control points. Food quality control is conducted at these check points to monitor the food production process (FAO/WHO, 2003)**.** Indeed, food quality control is applied throughout the entire food system to maintain a high standard of food quality control, which depends on the methods selected during food supply all the way to distribution. Quality control monitors the product itself, as well as the way it is produced, stored and transported. It is used to predict the quality of processed and/or storage foods and to control the process so the expected quality is achieved in every batch. In general, the food industry faces major challenges in terms of increasing the production efficiency while maintaining or improving the quality and safety of products. Thus, quality control procedures should be as simple as possible while providing the requisite information. Rapid and sensitive food analysis methodologies are useful tools for testing and ensuring the final product quality, especially for industrial applications. These methods should not be time consuming or expensive. The results of quality control testing can save time and reduce costs during the long process of manufacturing and storage.

Many food analysis and testing methods are used but the combination of FTIR microspectroscopy measurement with a thermal analyzer is a unique analytical techniques in the food sciences. The use of coupled techniques can overcome several problems and provide better sensitivity, higher speed and more accurate analysis (Ibañez. and Cifuentes, 2001; Herrero et al., 2012; Ravelo-Pérez et al., 2009). DSC–FTIR microspectroscopy has been used extensively for investigations in the polymer and pharmaceutical sciences, but it has been applied rarely in the food sciences. In the food sciences, this coupled technique can simulate the cooking process and serve as an accelerated stability testing method. Thermal changes in the IR absorption bands directly reflect changes in the molecular chemical structure and physical state of food components. Given these advantages, this combined technique is a useful approach that may complement conventional thermal analytical instruments used by the food sciences.

In this review article, we demonstrated that the DSC–FTIR technique is a rapid, simple and powerful analytical tool with many applications in the food sciences. The technique was applied successfully to the following analyses: the simultaneous investigation of encapsulated squid oil stability; the dehydration and intramolecular condensation of a sweetener (APM); the dehydration, rehydration and solidification of trehalose and the online monitoring of the Maillard reaction between Glc/Asn in a solid state. This novel DSC–FTIR microscopic system provides a unique and useful tool for determining the temperature-dependent behaviour of micro-samples and it may be used as an accelerated stability testing method for predicting product stability directly. Further extensive applications of DSC–FTIR microspectroscopic systems in the food sciences can be expected in the near future.

Acknowledgements

The authors thank Prof. L. S. Hwang, Prof. D. F. Hwang, and Dr. Yih-Dih Cheng for their helpful discussion, and Mr. J. L. Chien, Mr. Po-Chun Hsu, Miss T. F. Hsieh and Miss Ying-Ting Chi for their contributions on technical assistance, and Miss Y. T. Huang for figures drawing. The DSC–FTIR studies were financially supported by
National Science Council, Taipei, Taiwan, ROC and the Wei-Chuan Corp., Taiwan, ROC.

References

Akao, K., Okubo, Y., Ikeda, T., Inoue, Y., and Sakurai, M. (1998). Infrared spectroscopic study on the structural property of a trehalose water complex. *Chem. Lett.* 759-760.

Akao, K., Okubo, Y., Asakawa, N., Inoue, Y., and Sakurai, M. (2001). Infrared spectroscopic study on the properties of the anhydrous form II of trehalose. Implications for the functional mechanism of trehalose as a biostabilizer. *Carbohydr Res.* **334**: 233-241.

Akinade, K.A., Campbell, R.M., and Compton, A.C. (1994). The use of a simultaneous TGA/DSC/FT-IR system as a problem-solving tool. *J. Mater. Sci.* **29**: 3802-3812.

Alli, I. (2003). Food Quality Assurance: Principles and Practices. RC Press, Boca Raton, Florida, USA.

Belitz, H.-D., Grosch, W., and Schieberle, P. (2009). Food Chemistry, 4th Ed., Springer-Verlag, Berlin, Germany.

Bell, L.N. and Hageman, M.J. (1994). Differentiating between the Effects of Water Activity and Glass Transition Dependent Mobility on a Solid State Chemical Reaction: Aspartame Degradation. *J. Agric. Food Chem.*, **42**: 2398-2401.

Bell, L.N. and Labuza, T.P. (1991a). Aspartame degradation kinetics as affected by pH in intermediate and low moisture food systems. *J. Food Sci.* **56**: 17-20.

Bell, L.N. and Labuza, T.P. (1991b). Aspartame degradation as a function of "water activity". *Adv Exp Med Biol.* **302**: 337-349.

Berset, J.D. and Ochsenbein, N. (2012). Stability considerations of aspartame in the direct analysis of artificial sweeteners in water samples using high-performance liquid chromatography-tandem mass spectrometry (HPLC-MS/MS). *Chemosphere.* **88**: 563-569.

Boran, G., Karaçam, H., and Boran, M. (2006) Changes in the quality of fish oils due to storage temperature and time. *Food Chem.* 98**: 693-698.**

Butchko, H.H. and Stargel, W.W. (2001). Aspartame: scientific evaluation in the postmarketing period. *Regul. Toxicol. Pharmacol.* **34**: 221-233.

Chaiyasit, W., Elias, R.J., McClements, D.J., and Decker, E.A. (2007). Role of physical structures in bulk oils on lipid oxidation. *Crit. Rev. Food Sci. Nutr.* **47**: 299-317.

Cheng, Y.D. and Lin, S.Y. (2000). Isothermal Fourier transform infrared microspectrosopic studies on the stability kinetics of solid-state intramolecular cyclization of aspartame sweetener. *J. Agric. Food Chem*. **48**: 631-635.

Chuyen, N.V. (1998). Maillard reaction and food processing. Application aspects. *Adv. Exp. Med. Biol*. **434**:213-235.

Clute, M. (2008). Food Industry Quality Control Systems. CRC Press, Boca Raton, Florida, USA.

Cordella, C., Moussa, I., Martel, A.C., Sbirrazzuoli, N., and Lizzani-Cuvelier, L. (2002). Recent developments in food characterization and adulteration detection: technique-oriented perspectives. *J. Agric. Food Chem*. **50**: 1751-1764.

Coultate, T.P. (2009). Food: The Chemistry of Its Components. 5th ed., RSC Publishing, Cambridge, UK.

Crowe, J.H. (2007). Trehalose as a chemical chaperone: fact and fantasy. *Adv. Exp. Med. Biol.* **594**: 143-158.

Damodaran, S., Parkin, K.L., and Fennema, O.R. (2007). Fennema's Food Chemistry, Fourth Edition, CRC Press, Boca Raton, Florida, USA.

Devlin, J.P. (1990). Vibrational modes of amorphous ice: bending mode frequencies for isotopically decoupled H2O and HOD at 90K. *J. Mol. Struc.* **224**: 33-48.

Dziezak, J.D. (1986). Sweetners and product development. *Food Technol.* **40**: 111-130.

Earle, R.L. and Earle, M.D. (2003). Fundamentals of Food Reaction Technology. Leatherhead Publishing, Leatherhead, UK.

Elbein, A.D., Pan, Y.T., Pastuszak, I., and Carroll, D. (2003). New insights on trehalose: a multifunctional molecule. *Glycobiology.* **13**: 17R-27R.

El-Ghorab, A.H., Fujioka, K., and Shibamoto, T. (2006). Determination of acrylamide formed in asparagine/D-glucose maillard model systems by using gas chromatography with headspace solid-phase microextraction. *J. AOAC Int.* **89**: 149-153.

Eskin, M. and Robinson, D.S. (2000). Food Shelf Life Stability: Chemical, Biochemical, and Microbiological Changes. CRC Press, Boca Raton, Florida, USA.

FAO/WHO (2003). Assuring food safety and quality: Guidelines for strengthening national food control systems.

Farid, H.M. (2010). Mathematical Modeling of Food Processing. CRC Press, Boca Raton, Florida, USA.

Fay, L.B. and Brevard, H. (2005). Contribution of mass spectrometry to the study of the Maillard reaction in food. *Mass Spectrom. Rev.* **24**: 487-507.

Fellows, J.W., Chang, S.W., and Shazer, W.H. (1991). Stability of aspartame in fruit preparations used in yogurt. *J. Food Sci.* **56**: 689-691.

Fereidoon, S. (2005). Bailey's Industrial Oil and Fat Products: Volume 4. Edible Oil and Fat Products: Products and Applications (6th ed.), John Wiley and Sons, Inc.,New York, NY, USA.

Franks, F. (1994). Accelerated stability testing of bioproducts: attractions and pitfalls. *Trends Biotechnol.* **12**:114-117.

Furuki, T., Oku, K., and Sakurai, M. (2009). Thermodynamic, hydration and structural characteristics of alpha,alpha-trehalose. *Front. Biosci.* **14**: 3523-3535.

Giguere, P.A. (1987). The bifurcated hydrogen-bond model of water and amorphous ice. *J. Chem. Phys.* **87**: 4835-4839.

Gonzalez, M.J. (1995). Fish oil, lipid peroxidation and mammary tumor growth. *J. Am. Coll. Nutr.* **14**: 325-335.

Halim, S.A. and Newby, L.K. (2012). Review: Omega-3 fatty acid supplements provide no protective benefit in cardiovascular disease. *Ann. Intern. Med.* **157**: JC2-JC3.

Herrero, M., Simó, C., García-Cañas, V., Ibáñez, E., and Cifuentes, A. (2012). Foodomics: MS-based strategies in modern food science and nutrition. *Mass Spectrom. Rev.* **31**: 49-69.

Hodge, J.E. (1953). Chemistry of browning reactions in model systems. *J. Agric. Food Chem.* **1**: 928–943.

Hoenicke, K. and Gatermann, R. (2005). Studies on the stability of acrylamide in food during storage. *J. AOAC Int.* **88**: 268-273.

Huang T.C., Soliman, A.A., Rosen, R.T., and Ho C.T. (1987). Studies on the Maillard browning reaction between aspartame and glucose. *Food Chem.* **24**: 187-196.

Hwang, D.F., Hsieh, T.F., Hsu, P.C., Chi, Y.T., and Lin, S.Y. (2012). One-step simultaneous DSC-FTIR microspectroscopy to quickly detect continuous pathways in solid-state glucose/asparagine Maillard reaction. *Submitted for publication*

Ibañez, E. and Cifuentes, A. (2001). New analytical techniques in food science. *Crit. Rev. Food Sci. Nutr.* **41**: 413-450.

Johnson, D.J., Compton, D.A.C., and Canale, P.L. (1992). Applications of simultaneous DSC/FTIR analysis. *Thermochim. Acta.* **195**: 5-20.

Kaletunc, G. (2009). Calorimetry in Food Processing: Analysis and Design of Food Systems. Wiley-Blackwell, Ames, Iowa, USA.

Khan, A.A., Stocker, B.L., and Timmer, M.S. (2012). Trehalose glycolipids-- synthesis and biological activities. *Carbohydr. Res.* **356**: 25-36.

Kilcast, D. and Subramaniam, P. (2000). The Stability and Shelf-life of Food. Woodhead Pub., Cambridge, UK.

Kubow, S. (1990). Toxicity of dietary lipid peroxidation products. *Trends Food Sci. Technol.* **1**: 67-71.

Kulesza, K., Pielichowski, K., and German, K. (2006).Thermal decomposition of bisphenol A-based polyetherurethanes blown with pentane. *J. Anal. Applied Pyrolysis*. **76**: 243-248.

Lagouri, V. and Boskou, D. (1996). Nutrient antioxidants in oregano. *Int. J. Food Sci. Nutr.* **47**: 493-497.

Lee, J.H., O'Keefe, J.H., Lavie, C.J., and Harris, W.S. (2009) Omega-3 fatty acids: cardiovascular benefits, sources and sustainability. *Nat. Rev. Cardiol.* **6**: 753-758.

Leung, S.S. and Grant, D.J. (1997). Solid state stability studies of model dipeptides: Aspartame and aspartylphenylalanine. *J. Pharm. Sci.* **86**: 64-71.

Leung, S.S., Padden, B.E., Munson, E.J., and Grant, D.J. (1998a). Solid-state characterization of two polymorphs of aspartame hemihydrate. *J. Pharm. Sci*. **87**: 501-507.

Leung, S.S., Padden, B.E., Munson, E.J., and Grant, D.J. (1998b). Hydration and dehydration behavior of aspartame hemihydrate. *J. Pharm. Sci*. **87**: 508-513.

Lin, C.C. and Hwang, L.S (1993). Effects of tocopherol, β-carotene and ascorbyl palmitate on the oxidative stability of squid visceral oil, *J. Chin. Agric. Chem. Soc.* **31**: 365-377.

Lin, C.C. and Hwang, L.S. (2002). A Comparison of the Effects of Various Purification Treatments on the Oxidative Stability of Squid Visceral Oil. *J. AOCS.* **79**, 489-494

Lin, C.C., Lin, S.Y., and Hwang L.S. (1995a). Microencapsulation of squid oil with hydrophilic macromolecules for oxidative and thermal stabilization. *J. Food Sci.* 60: 36-39.

Lin, S.Y. and Cheng, Y.D. (2000). Simultaneous formation and detection of the reaction products of solid-state aspartame sweeteener by FT-IR/DSCmicroscopic system, *Food Addit. Contam.* **17**: 821-827.

Lin, S.Y., Hwang, L.S., and Lin CC. (1995b). Thermal analyser and micro FT-IR/DSC system used to determine the protective ability of microencapsulated squid oil. *J. Microencapsul.* **12**: 165-172.

Lin, S.Y. and Chien, J.L. (2003). In vitro simulation of solid-solid dehydration, rehydration, and solidification of trehalose dihydrate using thermal and vibrational spectroscopic techniques. *Pharm. Res.* **20**: 1926-1931.

Lin, S.Y. and Wang, S.L. (2012). Advances in simultaneous DSC-FTIR microspectroscopy for rapid solid-state chemical stability studies: some dipeptide drugs as examples. *Adv. Drug Deliv. Rev*. **64**: 461-478.

Magnuson, B.A., Burdock, G.A., Doull, J., Kroes, R.M., Marsh, G.M., Pariza, M.W., Spencer, P.S., Waddell, W.J., Walker, R., and Williams, G.M. (2007). Aspartame: a safety evaluation based on current use levels, regulations, and toxicological and epidemiological studies. *Crit. Rev. Toxicol.* **37**: 629-727.

Maqsood, S., Benjakul, S., and Kamal-Eldin, A. (2012). Extraction, processing, and stabilization of health-promoting fish oils. *Recent Pat. Food Nutr. Agric.* **4**: 141-147.

Martins, S.I.F.S., Jongen, W.M.F., and van Boekel, M.A.J.S. (2001). A review of Maillard reaction in food and implications to kinetic modelling. *Trends Food Sci. Technol.* **11**: 364–373.

Mirabella, F.M. (1986). Simultaneous differential scanning calorimetry (DSC) and infrared spectroscopy using an infrared microsampling accessory (IRMA) and FT-IR. *Appl. Spectrosc.* **40**: 417-420.

Muller, A and Steinhart, H. (2007). Recent developments in instrumental analysis for food quality. *Food Chem.* **102**: 436-444.

Ohtake, S. and Wang, Y.J. (2011). Trehalose: current use and future applications. *J Pharm Sci.* 100: 2020-2053.

Paré, J.R.J. and Bélanger, J.M.R. (1997). Instrumental methods in food analysis. *Tech. Instru. Anal. Chem.* **18**: 1-487.

Pattanaargson, S. and Sanchavanakit, C. (2000). Aspartame degradation study using electrospray ionization mass spectrometry. *Rapid Commun. Mass Spectrom*. **14**: 987-993.

Perjési, P., Pintér, Z., Gyöngyi, Z., and Ember, I. (2002). Effect of rancid corn oil on some onco/suppressor gene expressions in vivo. A short-term study. *Anticancer Res*. **22**: 225-230.

Pollien, P., Lindinger, C., Yeretzian, C., and Blank, I. (2003). Proton transfer reaction mass spectrometry, a tool for on-line monitoring of acrylamide formation in the headspace of maillard reaction systems and processed food. *Anal. Chem*. **75**: 5488-5494.

Prodolliet, J. and Bruelhart, M. (1993). Determination of aspartame and its major decomposition products in foods. *J. AOAC Int.* **76**: 275-282.

Ragnarsson, J.O. and Labuza, T.P. (1977) Accelerated shelf-life testing for oxidative rancidity in foods- a review. *Food Chem*. **2**: 291-308.

Ravelo-Pérez, L.M., Asensio-Ramos, M., Hernández-Borges, J., and Rodríguez-Delgado, M.A. (2009). Recent food safety and food quality applications of CE-MS. *Electrophoresis.* **30**: 1624-1646.

Rosén, J. and Hellenäs, K.E. (2002). Analysis of acrylamide in cooked foods by liquid chromatography tandem mass spectrometry. *Analyst*. **127**: 880-882.

Rossi, P.C., Pramparo, Mdel C., Gaich, M.C., Grosso, N.R., and Nepote, V. (2011). Optimization of molecular distillation to concentrate ethyl esters of eicosapentaenoic (20:5 ω-3) and docosahexaenoic acids (22:6 ω-3) using simplified phenomenological modeling. *J. Sci. Food Agric*. **91**: 1452-1458.

Sabah, S. and Scriba, G.K. (1998). Determination of aspartame and its degradation and epimerization products by capillary electrophoresis. *J. Pharm. Biomed. Anal.* **16**: 1089-1096.

Sakurai, M., Furuki, T., Akao, K., Tanaka, D., Nakahara, Y., Kikawada, T., Watanabe, M., and Okuda, T. (2008). Vitrification is essential for anhydrobiosis in an African chironomid, Polypedilum vanderplanki. *Proc. Natl. Acad. Sci. U S A.* **105**: 5093-5098.

Skibsted, L.H., Risbo, J., and Andersen, M.L. (2010). Chemical deterioration and physical instability of food and beverages. Woodhead Pub., Cambridge, UK.

Skwierczynski, R.D. and Connors, K.A. (1993). Demethylation kinetics of aspartame and L-phenylalanine methyl ester in aqueous solution. *Pharm. Res.* **10**: 1174-1180.

Soffritti, M., Belpoggi, F., Esposti, D.D., Lambertini, L., Tibaldi, E., and Rigano, A. (2006). First experimental demonstration of the multipotential carcinogenic effects of aspartame administered in the feed to Sprague-Dawley rats. *Environ. Health Perspect.* **114**: 379-385.

Sola-Penna, M. and Meyer-Fernandes, J.R. (1998). Stabilization against thermal inactivation promoted by sugars on enzyme structure and function: why is trehalose more effective than other sugars? *Arch Biochem. Biophys.* **360**: 10-14.

Spragg, R.A. (2000). Combining FTIR microspectroscopy with differential scanning calorimetry. *Analusis*. **28**: 64-67.

Staprans, I., Pan, X.M., Rapp, J.H., and Feingold, K.R. (2005). The role of dietary oxidized cholesterol and oxidized fatty acids in the development of atherosclerosis. *Mol. Nutr. Food Res.* **49**: 1075-1082.

Swanson, D., Block, R., and Mousa, S.A. (2012). Omega-3 fatty acids EPA and DHA: health benefits throughout life. *Adv. Nutr.* **3**: 1-7.

Sussich, F., Skopec, C., Brady, J., and Cesàro, A. (2001). Reversible dehydration of trehalose and anhydrobiosis: from solution state to an exotic crystal? *Carbohydr. Res.* **334**: 165-176.

Takanobu, H. (2002). Novel functions and applications of trehalose. *Pure Appl. Chem.* **74**: 1263-1269.

Taneja, A. and Singh, H. (2012) Challenges for the delivery of long-chain n-3 fatty acids in functional foods. *Annu, Rev, Food Sci, Technol.* **3**:105-123.

Valentas, K.J., Rotstain, E., and Singh, R.P. (1997). Handbook of Food Engineering Practice. CRC Press, Boca Raton, Florida, USA.

Vlachos, N., Skopelitis, Y., Psaroudaki, M., Konstantinidou, V., Chatzilazarou, A., and Tegou, E. (2006). Applications of Fourier transform-infrared spectroscopy to edible oils. *Anal. Chim. Acta.* **573-574**: 459-465.

Wnorowski, A. and Yaylayan, V.A. (2003). Monitoring carbonyl-amine reaction between pyruvic acid and alpha-amino alcohols by FTIR spectroscopy--a possible route to Amadori products. *J. Agric. Food Chem.* **51**: 6537-6543.

Yaylayan, V. (2009). Acrylamide formation and its impact on the mechanism of the early Maillard reaction. *J. Food Nutr. Res.* **48**: 1-7.

Yaylayan, V.A. and Stadler, R.H. (2005). Acrylamide formation in food: a mechanistic perspective. *J. AOAC Int.* **88**: 262-267.

Ziegler, B., Herzog, K., and Salzer, R. (1995). In-situ investigations of thermal processes in polymers by simultaneous differential scanning calorimetry and infrared spectroscopy. *J. Mol. Struct.* **348**: 457-460.

Figure Legends

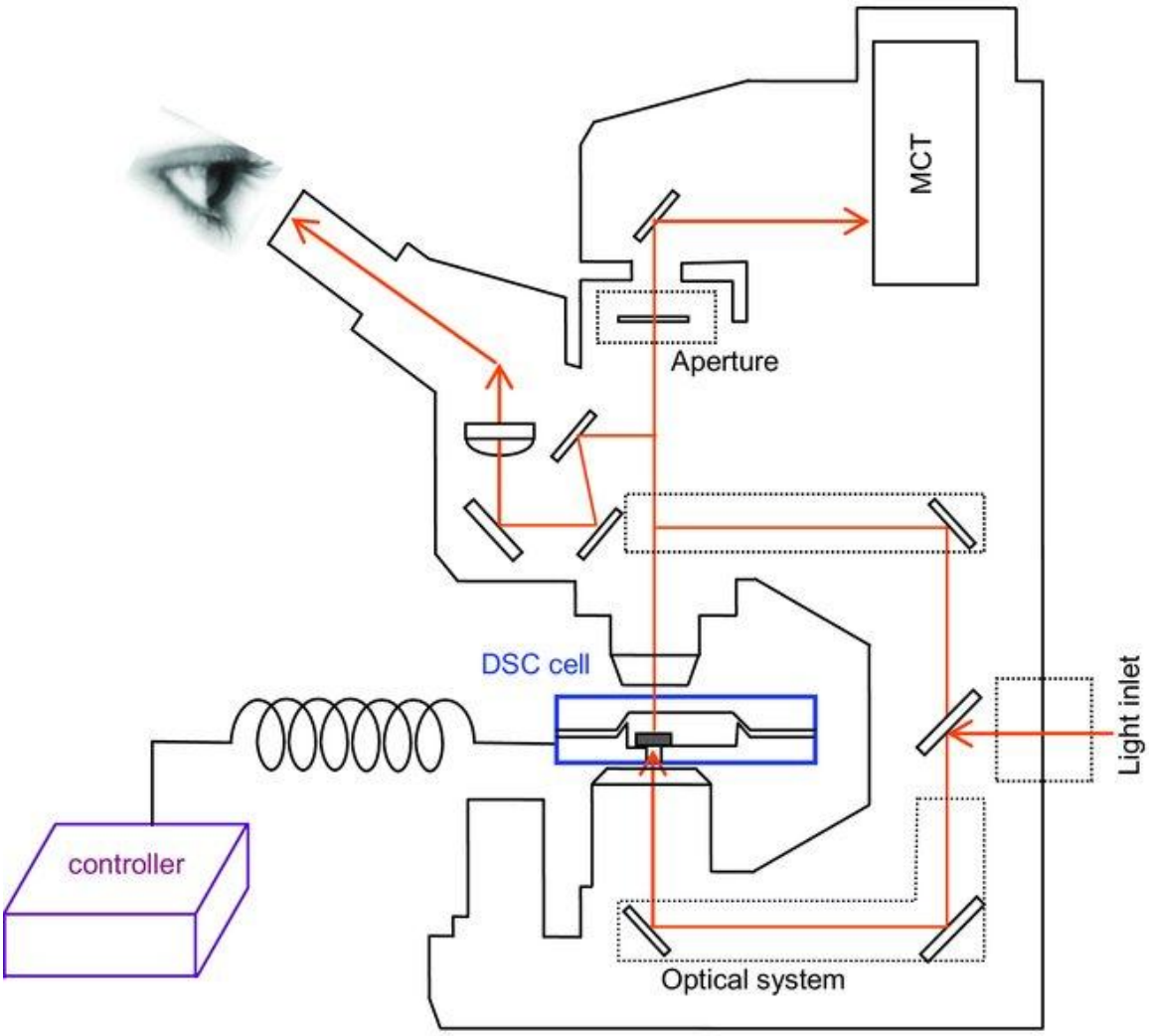

Fig. 1 Schematic diagram of the IR bean path through DSC-FTIR microspectroscopic apparatus.

Fig. 2

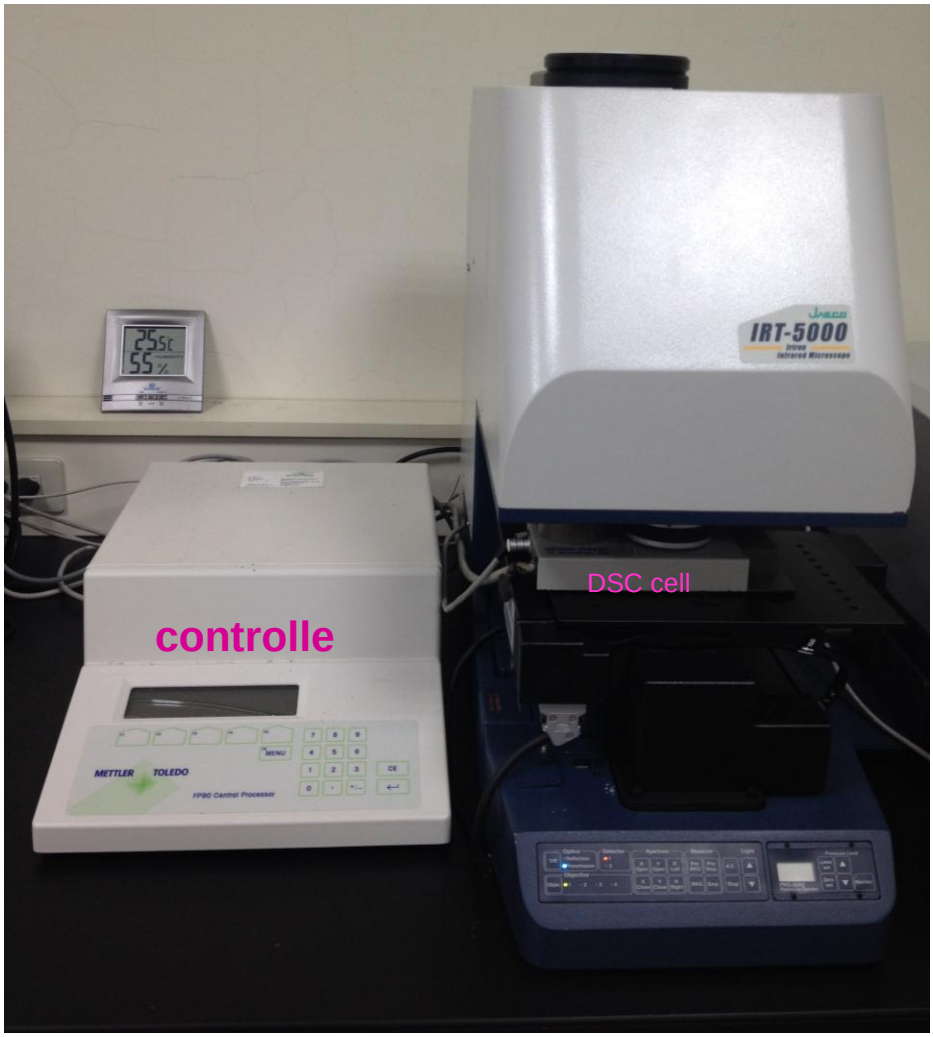

Fig. 2 Photograph of a DSC-FTIR microspectroscopic apparatus.

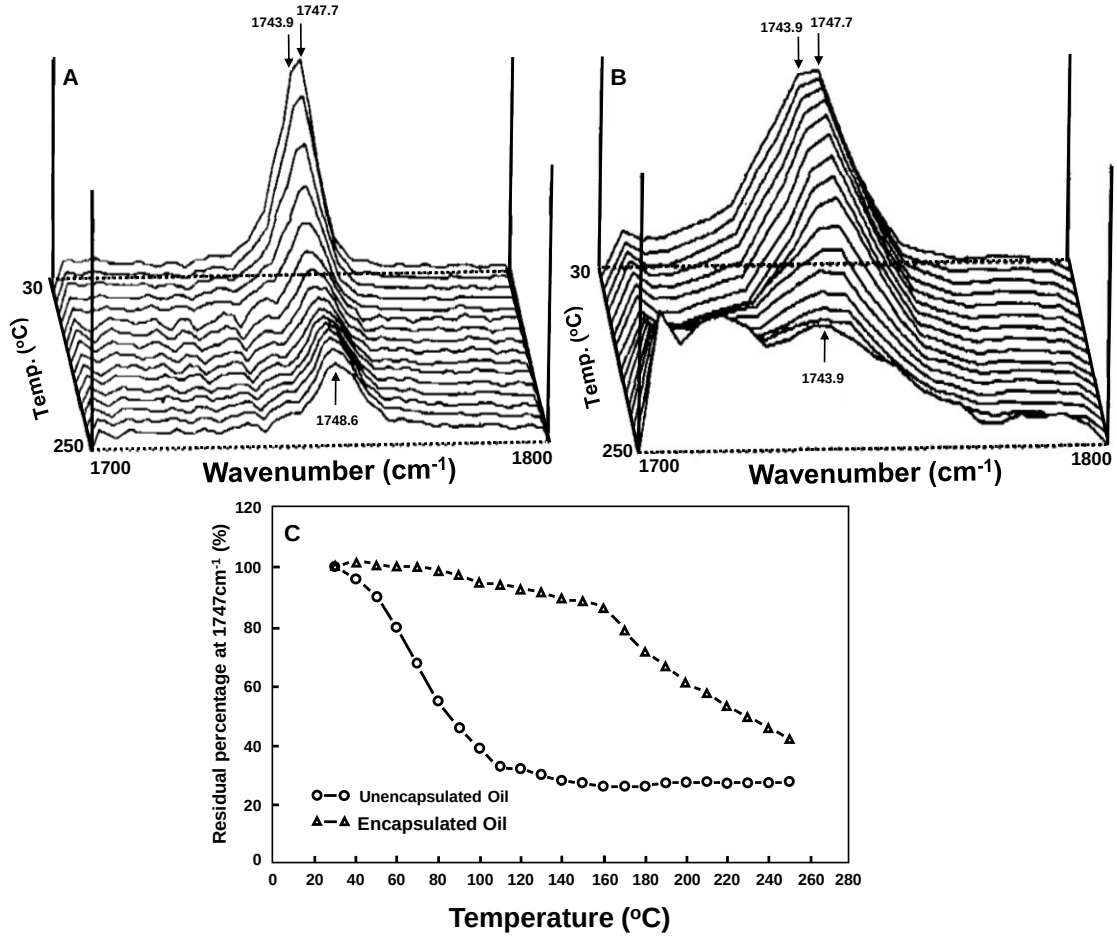

Fig. 3 Three-dimensional plot of FTIR spectra of the unencapsulated (A) or encapsulated (B) squid oil samples between 1700 and 1800 cm^{-1} as a function of temperature, and the change in peak intensity at 1747cm^{-1} with temperature (C).

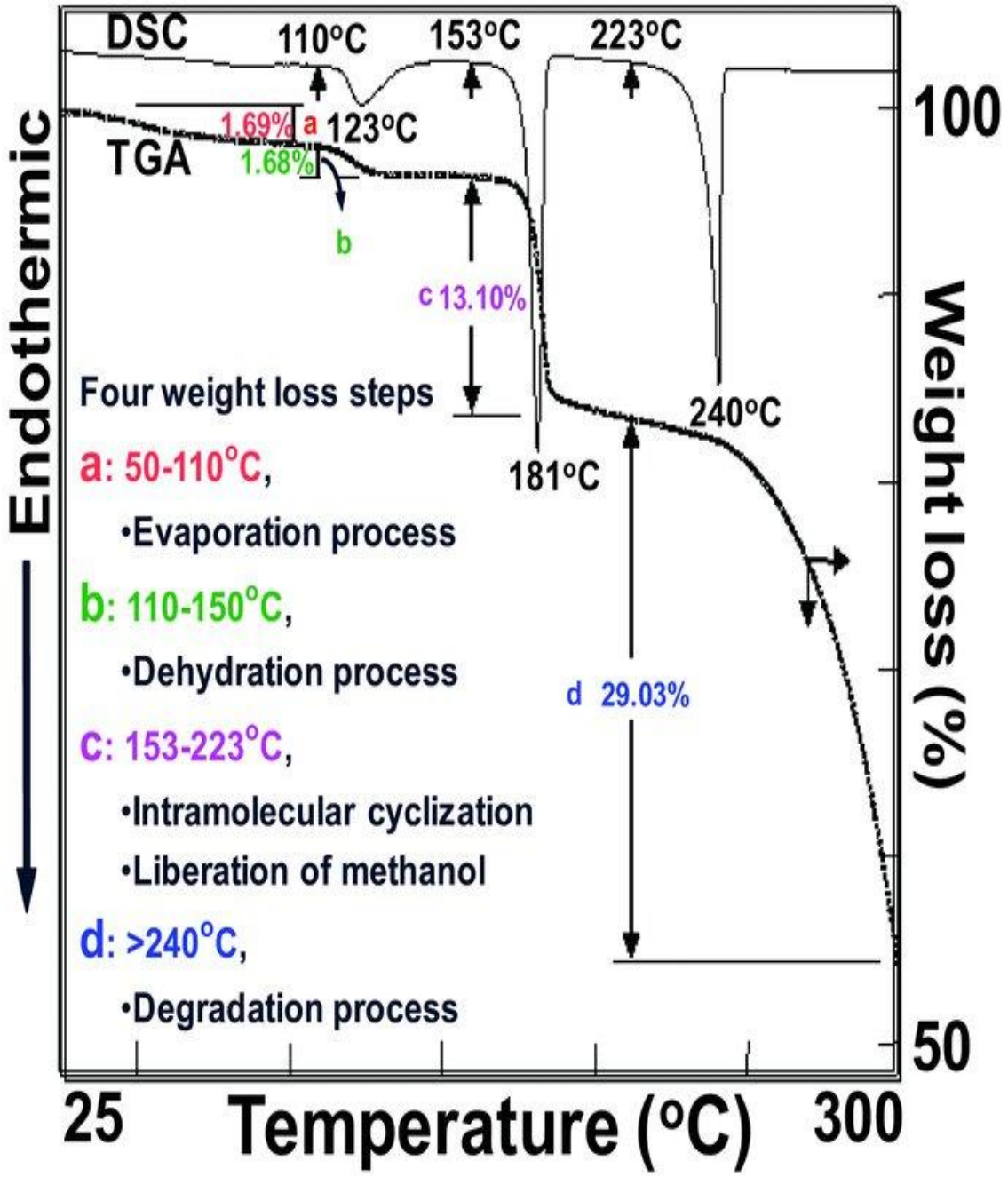

Fig. 4 DSC and TGA curves of APM hemihydrate.

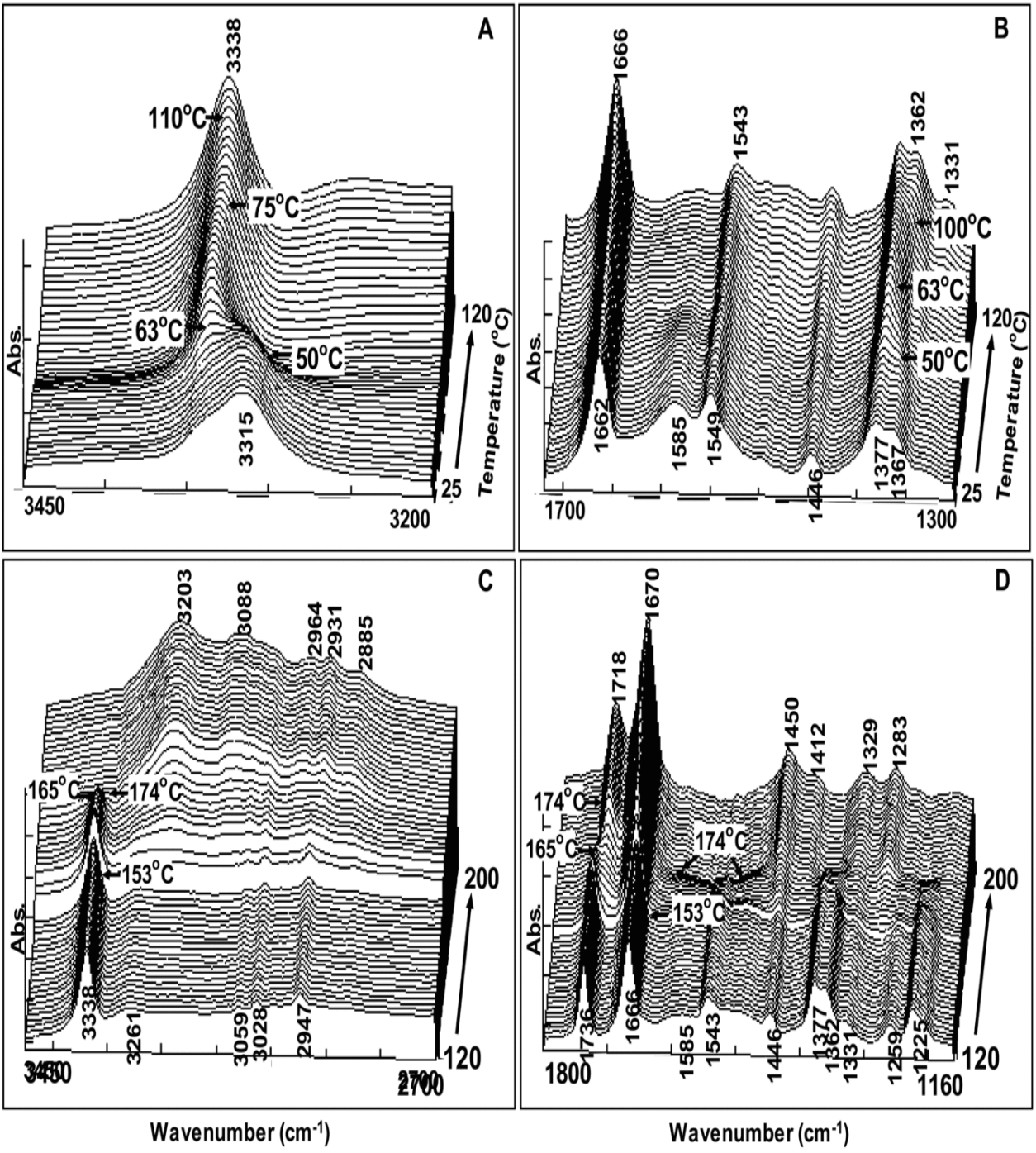

Fig. 5 Three-dimensional FTIR spectral plots of APM hemihydrate with the increase of temperature from 25 to 200°C.

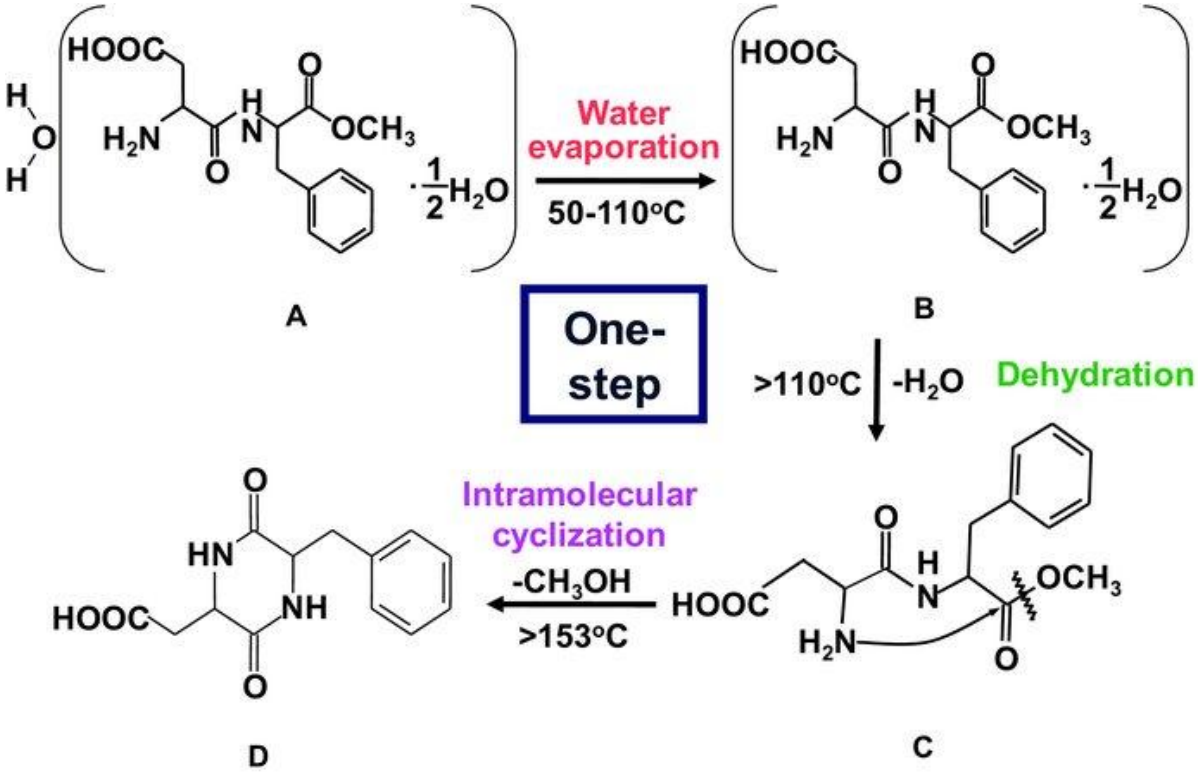

Fig. 6 The pathway of water evaporation, dehydration and intramolecular cyclization in solid-state APM hemihydrate.

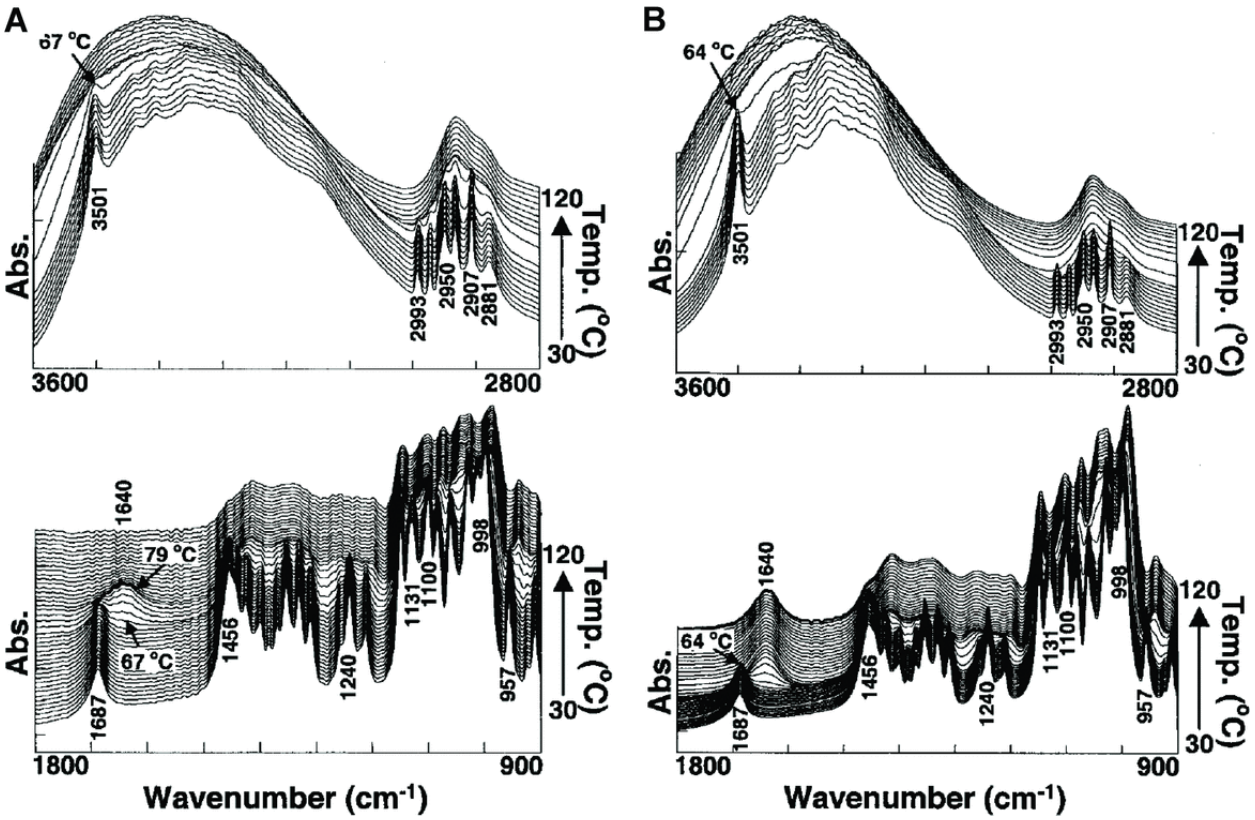

Fig. 7 Three-dimensional plots of the FTIR spectra of trehalose dihydrate prepared by the 1 KBr (A) or 2KBr (B) method within 3600-2800 cm^{-1} and 1800-900 cm^{-1}, as a function of temperature.

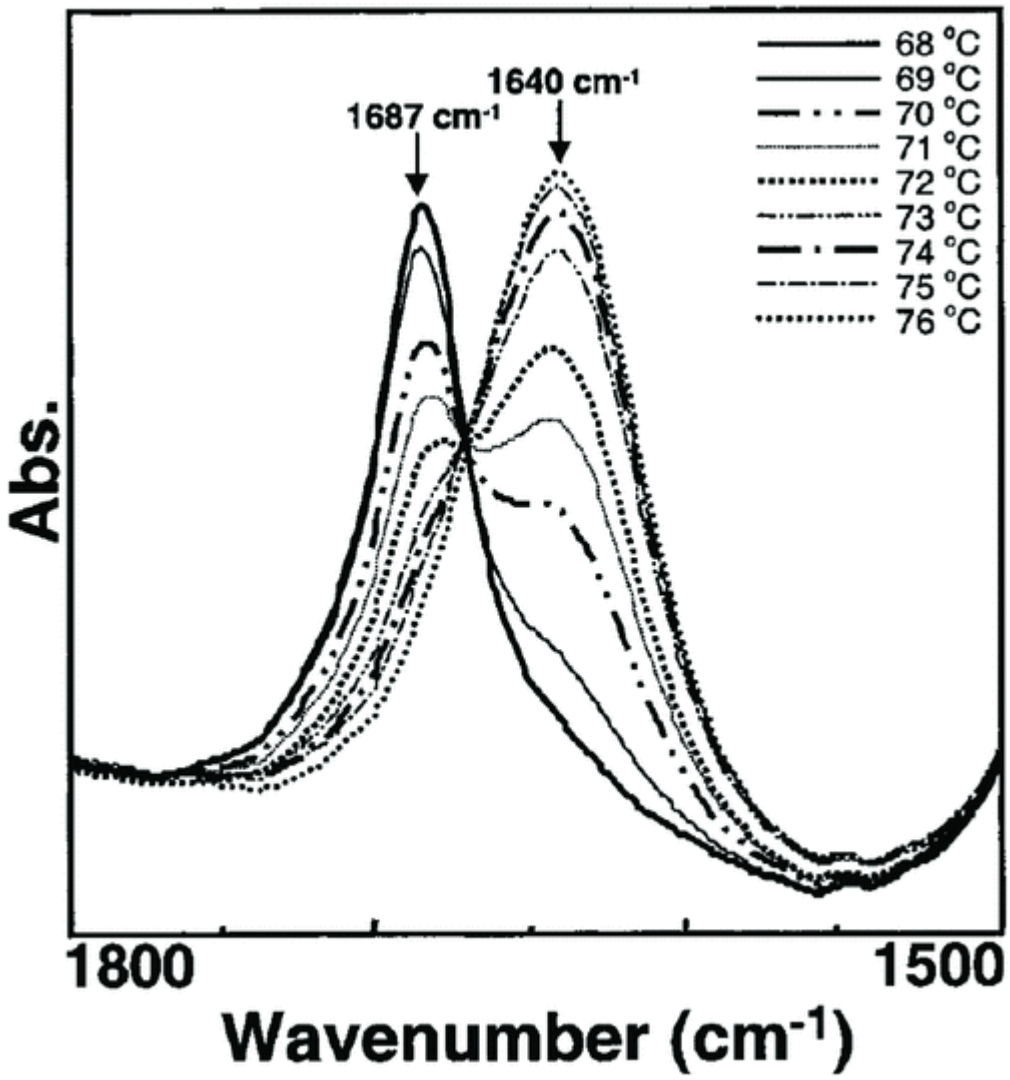

Fig. 8 Thermal-dependent changes in the FTIR spectral range of 1800-1500 cm^{-1} for trehalose dihydrate prepared by the 2KBr method.

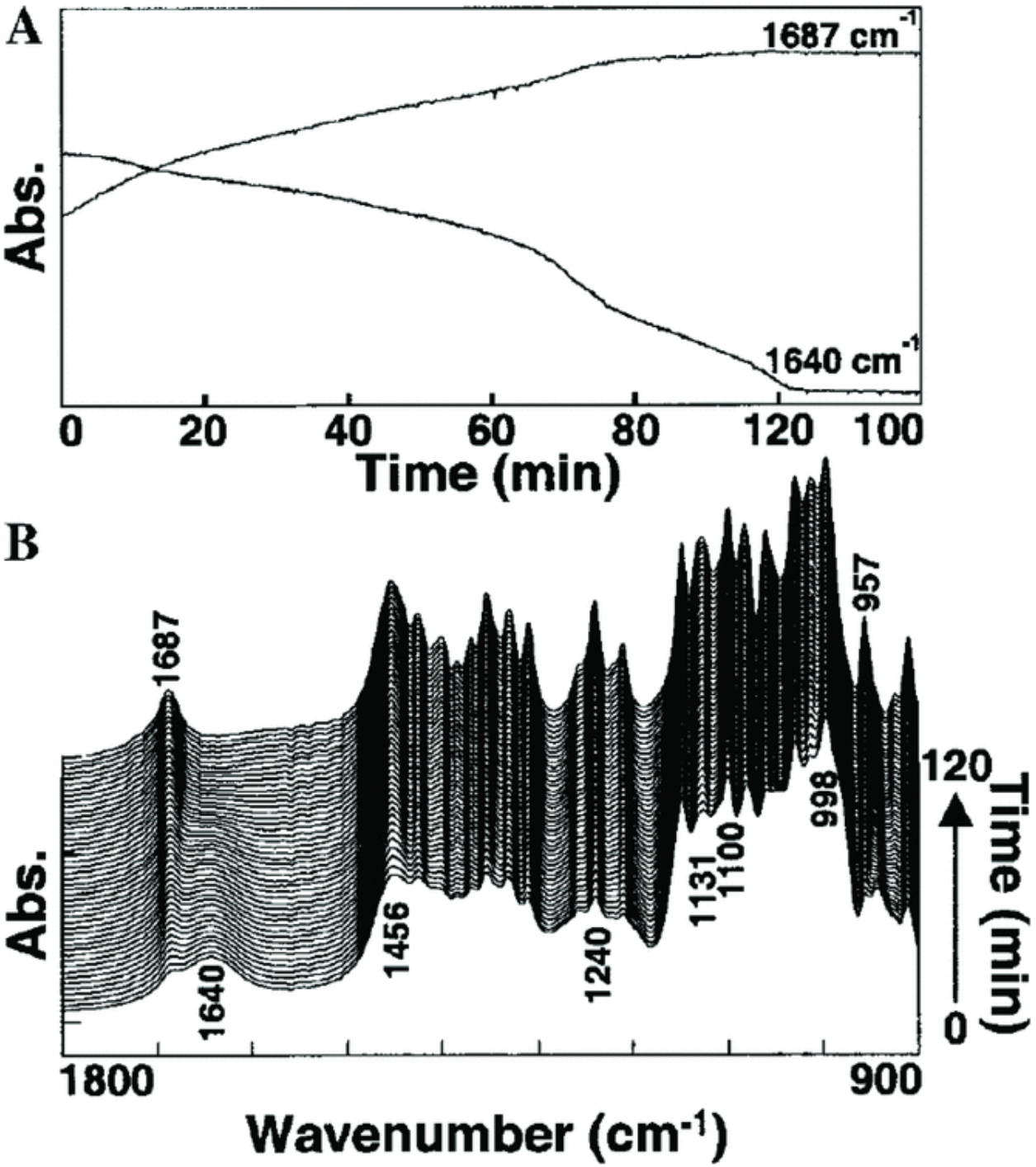

Fig. 9 Isothermal three-dimensional FTIR spectra of trehalose dihydrate preheated to 81°C followed cooling to 25°C, and isothermally studied at 25°C, 70% RH for 120 min.

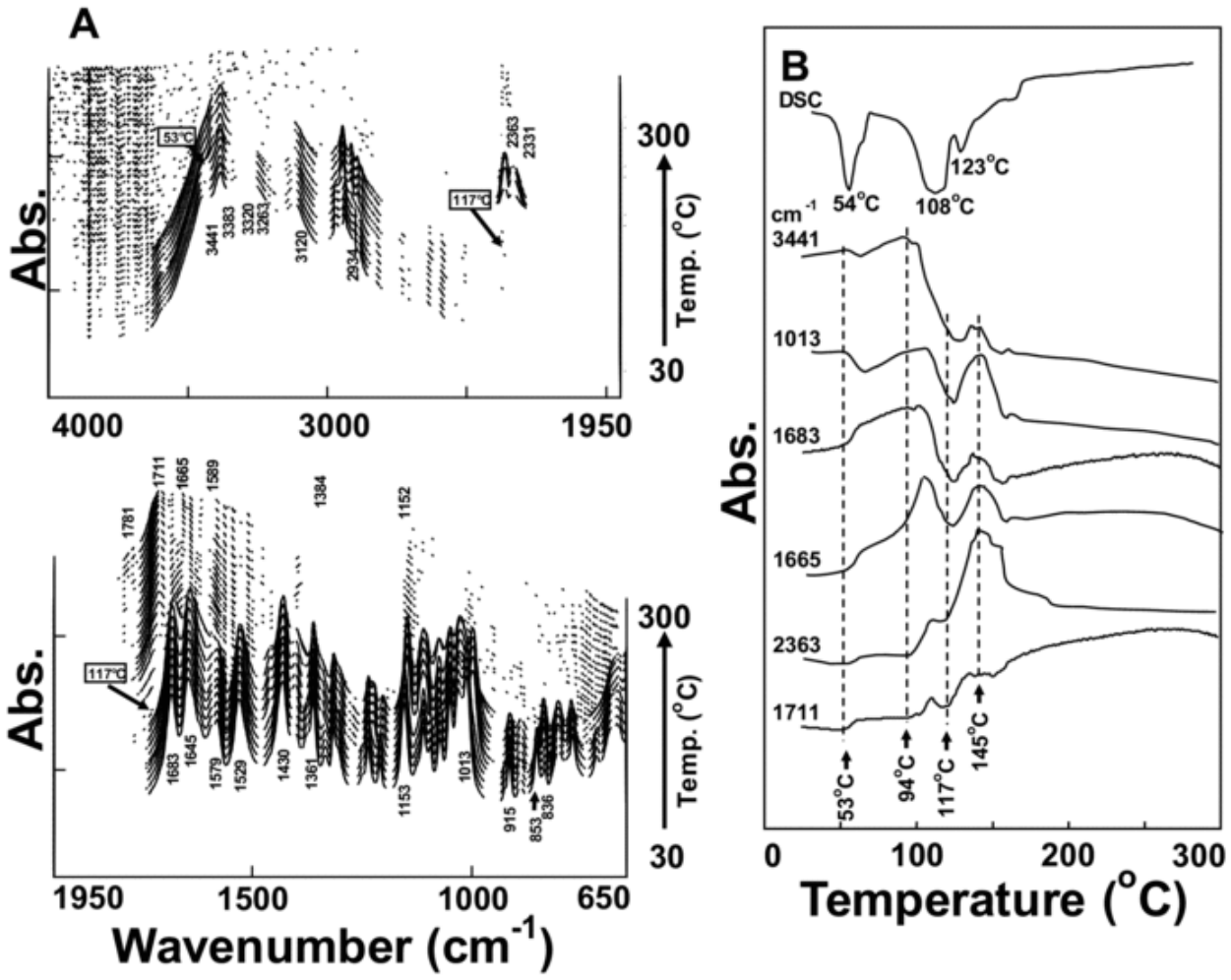

Fig. 10 Thermal-dependent three-dimensional FTIR spectral plot (A) and the changes in several specific IR peak intensities (B) for the physical mixture of Glu-Asn as a function of temperature.

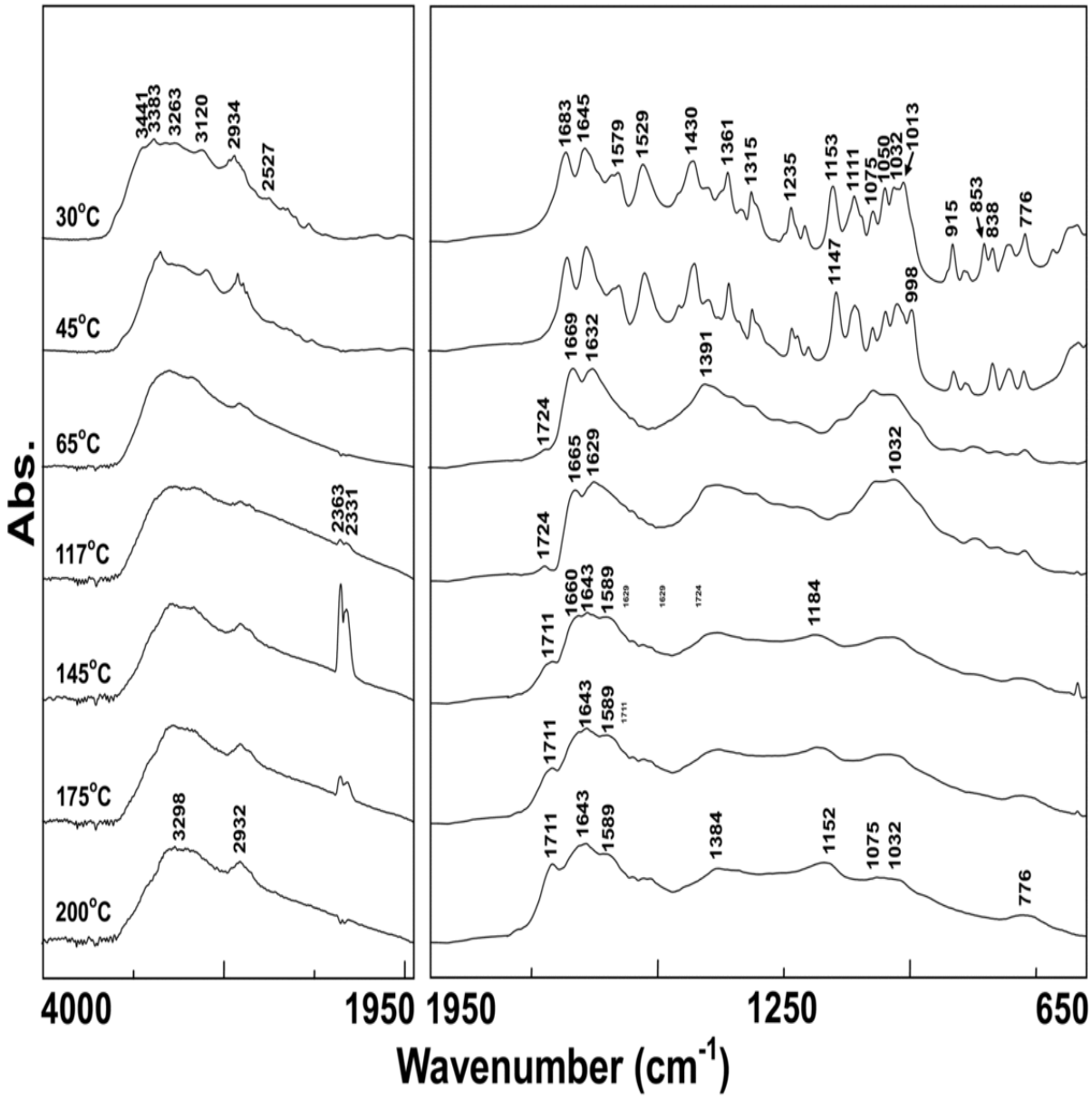

Fig. 11 FTIR spectra at each specific temperature from Fig. 10-A.

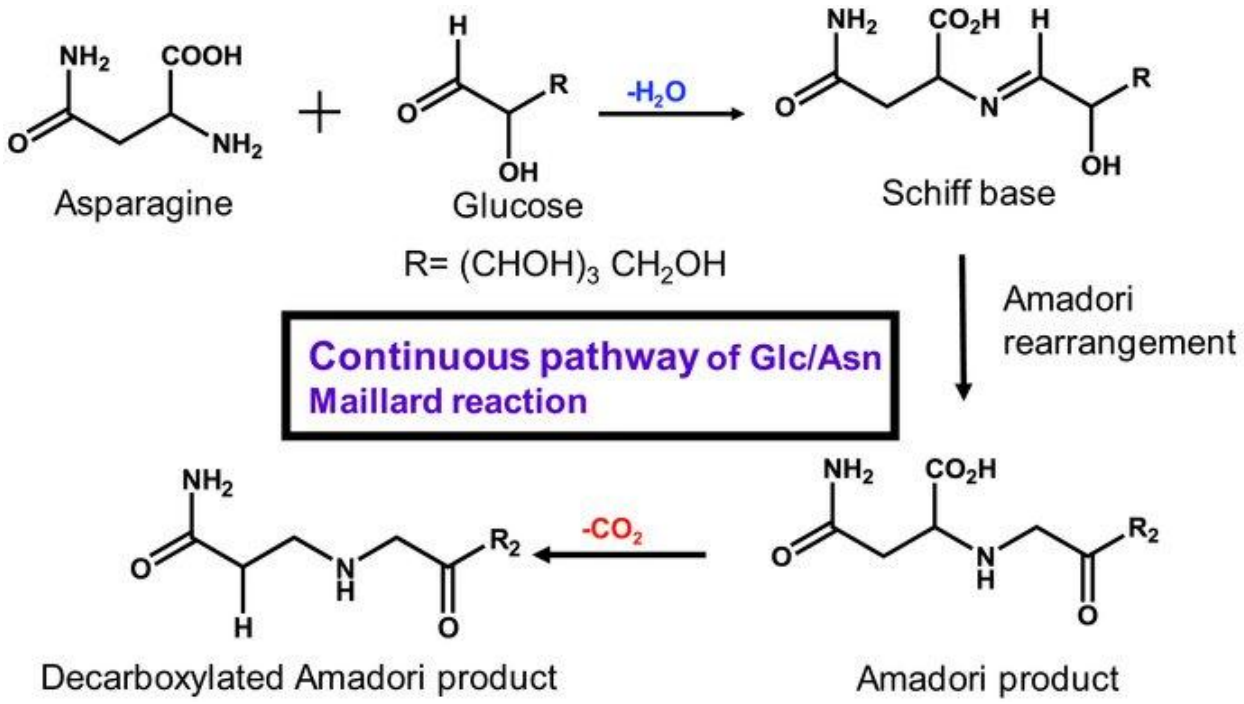

Fig. 12 The proposed mechanism for continuous pathway of Maillard reaction determined by simultaneous DSC-FTIR microspectroscopy.

Table I Analytical techniques usually used in food chemistry[a]

A. Spectroscopic Techniques

1. UV-Visible Spectroscopy

2. Infrared Spectroscopy (IR)

3. Raman Spectroscopy

4. Near Infrared Spectroscopy (NIR)

5. Nuclear Magnetic resonance (NMR)

6. Mass Spectrometry (MS)

7. Atomic Spectroscopy (AS)

B. Biological Techniques

1. Polymerase Chain Reaction (PCR)

2. Immunological Techniques

C. Separation Techniques

1. Gas Chromatography (GC)

2. Liquid Chromatography (LC)

3. Supercritical Fluid Chromatography (SFC)

4. Capillary Electrophoresis (CE)

D. Electrochemical Techniques

1. Biosensor

2. Immunochemical biosensor (ELISA)

E. Thermal Analysis

1. Differential Thermal Analysis (DTA)

2. Differential Scanning Calorimetry (DSC)

3. Thermogravimetry Analysis (TGA)

4. Dynamic Mechanical Analyzer (DMA)

5. Dynamic Vapor Sorption (DVS)

F. Coupled Techniques

1. CE-MS

2. GC-MS

3. GC-FTIR

4. GC-ICP-MS

5. HPLC-NMR

5. HPLC-MS

6. HPLC-ICP-MS

7. FIA-ICP-MS

8.SFC-MS

*ICP: Inductively Coupled Plasma

**FIA: Flow injection analysis

a: modified from Ibañez, E. and Cifuentes, A. (2001). *Crit. Rev. Food Sci. Nutr*. **41**: 413-450.